

The effect of HIF-1 α and PKM1 expression on acquisition of chemoresistance

Mitsuyoshi Okazaki¹
 Sachio Fushida¹
 Tomoya Tsukada¹
 Jun Kinoshita¹
 Katsunobu Oyama¹
 Tomoharu Miyashita¹
 Itasu Ninomiya¹
 Shinichi Harada²
 Tetsuo Ohta¹

¹Department of Gastroenterological Surgery, Division of Cancer Medicine, Graduate School of Medical Science, Kanazawa University, Ishikawa, Japan;

²Center for Biomedical Research and Education, School of Medicine, Kanazawa University, Ishikawa, Japan

Background: In patients with gastric cancer, one of the greatest obstacles to effective chemotherapy is the development of chemoresistance. It has been previously reported that hypoxia-inducible factor-1 alpha (HIF-1 α) is associated with acquisition of chemoresistance, and more recent studies have also noted an association of pyruvate kinase muscle 1 (PKM1) and chemoresistance. The purpose of this study was to identify the effect of HIF-1 α and PKM1 expression on the development of acquired chemoresistance using a paclitaxel (PTX)-resistant gastric cancer cell line.

Materials and methods: A cancer cell line resistant to PTX was established from MKN45 cells by stepwise exposure to drug (rMKN45-PTX). The expressions of HIF-1 α , apoptosis, vascular endothelial growth factor (VEGF), multidrug transporters and glycolytic enzyme were examined by Western blotting, enzyme-linked immunosorbent assay and immunohistochemistry. We also assessed the tumor proliferation by subcutaneous tumor and peritoneal dissemination of mouse xenograft model.

Results: The resistance index was 6.1 by determining as the ratio of the 50% growth inhibition (IC₅₀) of rMKN45-PTX/IC₅₀ of MKN45. Expression of nuclear factor kappa B and HIF-1 α was increased in rMKN45-PTX cells compared with the parent cells. Expression of Bax and caspase-3 was significantly downregulated, whereas expression of Bcl-xL, P-glycoprotein, multidrug resistance-associated protein and VEGF was increased in rMKN45-PTX. The expression level of PKM1 was upregulated in rMKN45-PTX, leading to an increase in the PKM1/PKM2 ratio. Using xenograft models, we demonstrated that mouse subcutaneous tumors derived from rMKN45-PTX were significantly larger than those derived from MKN45 cells.

Conclusion: Under the stress of chemotherapeutic agent exposure, high expression of HIF-1 α affects various downstream genes. Although the underlying mechanism is unknown, our data suggest that PKM1 is also a molecular target for gastric cancer treatment.

Keywords: HIF-1 α , PKM1, chemoresistance, gastric cancer

Introduction

Gastric cancer is the fourth most commonly diagnosed cancer and the second leading cause of cancer death worldwide.¹ Most patients in the advanced stages of disease are treated with chemotherapy to prolong their survival. However, even if the regimen is effective, the cancer becomes chemoresistant with repeated treatment² and new strategies to counter chemoresistance in gastric cancer are therefore required.

Acquisition of chemoresistance is a complex and multifactorial phenomenon related to the tumor microenvironment, and the mechanism has not been fully elucidated. Cancer cell lines with resistance to anticancer drugs can provide valuable model systems

Correspondence: Sachio Fushida
 Department of Gastroenterological Surgery, Division of Cancer Medicine, Graduate School of Medical Science, Kanazawa University, 13-1 Takara-machi, Kanazawa, Ishikawa 920-8641, Japan
 Email fushida@staff.kanazawa-u.ac.jp

to investigate the detailed molecular mechanisms. However, to date there have been few reports about the establishment of cancer cell lines resistant to anticancer drugs.³⁻⁶

Paclitaxel (PTX), a member of the taxane family, is a diterpenoid compound obtained from *Taxus brevifolia*.⁷ It disturbs depolymerization of microtubules in malignant cells⁸ and thereby inhibits cell division and triggers apoptosis.⁹ Because PTX is one of the most commonly used therapeutic agents in gastric cancer patients, it is necessary to develop new methods of overcoming resistance to PTX in clinical practice.

Previous experimental studies showed that hypoxia-inducible factor-1 alpha (HIF-1 α) may be a factor involved in acquisition of chemoresistance.¹⁰⁻¹⁶ In various cancer, HIF-1 α is the aryl hydrocarbon receptor nuclear translocator that forms a functional complex with β subunits under hypoxia, which transactivates more than 60 genes associated with angiogenesis, apoptosis and cell proliferation.¹⁰⁻¹²

Furthermore, nuclear factor kappa B (NF- κ B) also may be linked to chemoresistance.¹³ The NF- κ B family is composed of the transcription factors that regulate the HIF system (NF- κ B/HIF-1 α pathway).¹⁴ Liu et al demonstrated an association between HIF-1 α expression and activation of the NF- κ B signal pathway in chemoresistance acquisition using the vincristine-resistant gastric cancer cell line SGC7901/VCR.¹⁵ It was recently noted that genes related to cancer metabolism such as pyruvate kinase muscle 1 (PKM1) may also play an important role in chemoresistance acquisition.¹⁶

The purpose of this study was to elucidate the molecular mechanisms associated with HIF-1 α and PKM1 that lead to acquired chemoresistance using a newly established PTX-resistant gastric cancer cell line.

Materials and methods

Antineoplastic agent

PTX was kindly provided by Bristol-Myers Squibb Co. (Tokyo, Japan). PTX was reconstituted in distilled water at appropriate concentrations and stored at -20°C until use. The reagent was used as recommended by this supplier.

Cell lines and cell culture

The gastric cancer cell line used in this study was MKN45, which was purchased from American Type Culture Collection (Rockville, MD, USA). Cells were maintained in RPMI-1640 medium supplemented with 10% fetal bovine serum, penicillin (100 U/mL) and streptomycin (100 $\mu\text{g}/\text{mL}$). The cells were maintained in a humidified atmosphere of 5% CO_2 in air at 37°C .

Establishment of PTX-resistant cancer cell lines

PTX-resistant cells were established by exposure to increasing concentrations of PTX similar to the previously described method.⁴⁻⁶ MKN45 cells were initially cultured in RPMI containing PTX at a concentration of 0.1 nM and subsequently subcultured with increasing concentrations of PTX. Once surviving cells reached 80% confluence, they were passaged twice in the same concentration of PTX, after which the process was repeated with increasing doses of PTX until a cell population was selected that demonstrated more than three times of 50% growth inhibition (IC_{50}) to PTX than the parental cell line. The resultant cell line that grew under the high concentrations of PTX was made as a drug-resistant gastric cancer cell line and named rMKN45-PTX. rMKN45-PTX used in this study was selected from a culture dish almost 1 year later. Experiments were performed after culturing for 2 weeks under the absence of PTX.

3-(4,5-Dimethylthiazol-2-yl)-2, 5-diphenyltetrazolium bromide (MTT) assay

The viability of cancer cells was determined by the MTT assay. Cells were seeded at 4×10^3 per well in 96-well plates and incubated overnight at 37°C in a humidified environment containing 5% CO_2 . PTX was dissolved in phosphate-buffered saline (PBS) and added to the cell culture medium at various concentrations (0–100 nM). After 48 h of treatment, the supernatant was discarded and MTT solution was added to each well (500 $\mu\text{g}/\text{mL}$ final concentration) and incubated at 37°C for 3 h. Then, the supernatant was removed, and 150 μL of DMSO (Wako, Tokyo, Japan) was added. The absorbance of the solution was read at a wavelength of 535 nm using a microplate reader (Bio-Rad 550; Bio-Rad, Hercules, CA, USA). Cell viability was calculated as follows: viability = (absorbance of experimental wells)/(absorbance of control wells). All experiments were repeated at least three times. The IC_{50} of each chemotherapeutic drug was determined as the drug concentration showing 50% cell growth inhibition compared with the control cell growth. The resistance index (RI) was calculated as the IC_{50} of rMKN45-PTX/the IC_{50} of MKN45. Chemoresistance of cancer cell lines was defined by a RI of 3.0 or greater.

Flow cytometric analysis of cell cycle distribution

Single-cell suspension was collected, washed with cold PBS three times and fixed with 70% ethanol at 4°C overnight. After centrifugation, the supernatant was discarded and

the cells were washed twice with cold PBS. The cells were then stained with propidium iodide. The sub-G0/G1, S and G2/M phase fractions of 2×10^4 cells were determined by flow cytometry using a FACS Caliber (Becton Dickinson).

Western blotting

Approximately 5×10^6 cells were lysed in RIPA buffer containing 1% protease inhibitor cocktail (Sigma-Aldrich Co.). The protein concentration of each sample was measured using a BCA protein assay kit (Pierce Biotechnology, Waltham, MA, USA). In total, 20 μ g of protein from each sample was loaded onto 12.5% SDS-PAGE gels and subjected to electrophoresis. Proteins were transferred to polyvinylidene fluoride membranes (Bio-Rad Laboratories Inc., Hercules, CA, USA) and blocked with commercial gradient buffer (0.1% Tween-20; EZ Block; ATTO Corporation, Tokyo, Japan) at room temperature for 30 min. Blots were incubated overnight at 4°C with each primary antibody (see following text) and then incubated for 1 h with the appropriate horseradish peroxidase (HRP)-conjugated secondary antibodies. The antibody-antigen complexes were detected with an ECL Western blotting detection kit (GE Healthcare Japan Ltd., Japan) and a Light-Capture system (ATTO Corporation, NY, USA). To ensure equal protein loading, β -actin levels were measured using an anti- β -actin monoclonal antibody. We performed Western blot analysis by using same cell lysate. Primary antibodies against the following proteins were used: HIF-1 α (rabbit polyclonal IgG, diluted 1:500; Santa Cruz Biotechnology, Inc., Dallas, TX, USA), Bax (rabbit monoclonal IgG, diluted 1:200; Abcam, Cambridge, UK), Bcl-xL (rabbit monoclonal IgG, diluted 1:1000; Abcam), caspase-3 (rabbit polyclonal IgG, diluted 1:1000; Abcam), multidrug resistance-associated protein (MRP; mouse polyclonal IgG, diluted 1:500; Abcam), P-glycoprotein (P-gp; rabbit polyclonal IgG, diluted 1:1000; Abcam), PKM1 (rabbit polyclonal IgG, diluted 1:500; Novus Biologicals), PKM2 (rabbit polyclonal IgG, diluted 1:1000; Abcam), vascular endothelial growth factor (VEGF; rabbit polyclonal IgG, diluted 1:1000; Santa Cruz Biotechnology, Inc.) and β -actin (mouse monoclonal IgG, diluted 1:10,000; Sigma-Aldrich Co.).

Enzyme-linked immunosorbent assay (ELISA)

Serum-free conditioned media (SF-CM) was prepared from rMKN45-PTX and MKN45 cells as previously reported.¹⁷ Briefly, 1.0×10^6 cells were seeded into 100 mm tissue culture dishes with 10 mL RPMI supplemented with 10% FBS and incubated at 37°C for 3 days. To obtain SF-CM, the cells were

washed twice with PBS and then incubated for 2 days with 5 mL of serum-free RPMI. SF-CM was harvested, centrifuged at $1500 \times g$ for 5 min and passed through a filter (pore size: 0.45 μ m). The concentration of VEGF was measured by ELISA (Quantikine; R&D Systems, Wiesbaden, Germany) according to the manufacturer's instructions.

Mouse xenograft model

All animal experiments were performed according to standard guidelines of Kanazawa University. All procedures followed were in accordance with the ethical standards of the responsible committee on human experimentation (institutional and national) and with the Helsinki Declaration of 1964 and later versions. The study was approved by the Research Ethics Committee of Kanazawa University. Female immunocompromised BALB/c-nu/nu mice (Charles River Laboratories Inc., Yokohama-shi, Japan) aged 4–6 weeks were maintained in a sterile environment. For the subcutaneous model, a total of 5×10^6 MKN45 and rMKN45-PTX cells in 100 μ L of RPMI were subcutaneously injected into the dorsal side of each mouse on day 0. The left dorsal side was injected with MKN45 and the right side was injected with rMKN45-PTX. Animals were carefully monitored and tumors of five sample were measured every 4 days. The tumor volume (V) was calculated according to the formula $V = AB^2/2$, where A is the length of the major axis and B is the length of the minor axis. For the peritoneal dissemination model, 5×10^6 cells in 1,000 μ L of RPMI were intraperitoneally injected into nude mice on day 0. After 14 days, mice were anesthetized with diethyl-ether and sacrificed, and the tumors and abdominal organs were excised together. Tumor specimens were then collected for immunohistochemical examination.

Immunohistochemistry

Tumor specimens were fixed in 10% neutral buffered formalin and embedded in paraffin. The expression levels of NF- κ B p65 (mouse monoclonal IgG, diluted 1:100; Santa Cruz Biotechnology, Inc.), VEGF (rabbit polyclonal IgG, diluted 1:100; Santa Cruz Biotechnology, Inc.), Ki-67 (mouse monoclonal IgG, diluted 1:100; DakoCytomation, Glostrup, Denmark), PKM1 (rabbit polyclonal IgG, diluted 1:500; Novus Biologicals) and PKM2 (rabbit polyclonal IgG, diluted 1:1000; Abcam) were assessed immunohistochemically. Deparaffinized sections were pretreated by autoclaving in 10% citric acid buffer (pH 8.0) at 120°C for 15 min. Following treatment with protein block serum (DakoCytomation, Kyoto, Japan) for 10 min and incubation with 2% skim milk for 30 min to block non-specific reactions, sections

were incubated with primary antibody at 4°C overnight. The Envision-polymer solution (horseradish peroxidase, DakoCytomation) was then applied for 1 h. Sections were examined using a fluorescence microscope (Olympus, Tokyo, Japan). The Ki-67 index was calculated as a percentage of expression within the whole section in all samples using a BZ-9000 BZII microscope (Keyence, Osaka, Japan).

Statistical analysis

Values are expressed as mean \pm SD. Comparisons were made using one-way analysis of variance or Student's *t*-test using SPSS statistical software, version 11.0 (SPSS). In all analyses, $P < 0.05$ indicated statistical significance.

Results

Establishment of PTX-resistant gastric cancer cell line

To obtain a PTX-resistant cell line, MKN45 cells were treated with increasing concentrations of PTX up to 20 nM. The IC_{50} value of PTX for MKN45 was 5.9 nM. By contrast, the IC_{50} level for rMKN45-PTX was 36 nM. RI calculated as the ratio of the IC_{50} level of rMKN45-PTX/ IC_{50} of MKN45 was 6.1 (Figure 1, Table 1). Since the RI of rMKN45-PTX was greater than 3.0, this cell line was successfully established as a chemoresistant cancer cell line and was used for further investigation. Regarding morphologic appearance under a light microscope, rMKN45-PTX formed spheroid bodies, in contrast to MKN45 (Figure 2).

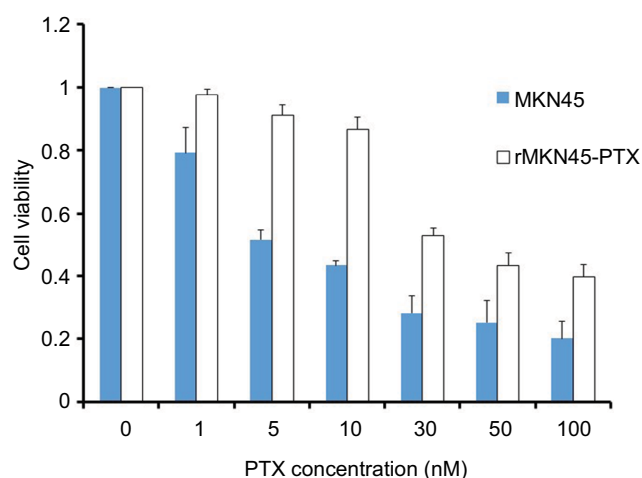


Figure 1 Drug sensitivity of rMKN45-PTX and MKN45 by MTT assay.

Note: Results are mean values from five experiments.

Abbreviations: MTT, 3-(4,5-dimethylthiazol-2-yl)-2, 5-diphenyltetrazolium bromide; PTX, paclitaxel.

Cell cycle distribution

Our results showed no significant differences between rMKN45-PTX and the parent cell line in the proportion of cells in G0/G1 phase (66.2% vs. 58.6%, N.S.) and G2/M phase (17.3% vs. 21.4%, N.S.) (Figure 3). Results are representative data of three different experiments.

Expression of HIF-1 α and chemoresistance-related proteins

Western blotting results revealed that the expression level of HIF-1 α in rMKN45-PTX was significantly higher than that in MKN45 as shown in Figure 4. rMKN45-PTX cells showed upregulation of the antiapoptotic protein Bcl-xL and downregulation of the proapoptotic protein Bax and the effector enzyme caspase-3 in comparison with the parental cells (Figure 5A). Also, the expression of P-gp, MRP and VEGF was increased in rMKN45-PTX compared with the parent cells (Figure 5A). We also used ELISA to measure the level of VEGF in the culture media and showed that rMKN45-PTX had elevated levels of VEGF compared with MKN45 (Figure 5B). The expression level of PKM1 was upregulated in rMKN45-PTX compared with the parent cells. By contrast, the expression level of PKM2 was almost identical to that of the parent cells (Figure 6A). As a result, the PKM1/PKM2 ratio was significantly increased in rMKN45-PTX (Figure 6B). β -Actin was used as an internal control loading in each lane. Results are representative data of three different experiments.

Table 1 Establishment of drug-resistant cancer cell line

Cell line	IC_{50}	Final concentration	RI
MKN45	5.9	–	–
rMKN45-PTX	36	20 nM	6.1

Notes: RI = IC_{50} of rMKN45-PTX/ IC_{50} of MKN45. “–” indicates data not available.

Abbreviations: IC_{50} , 50% growth inhibition; PTX, paclitaxel; RI, resistance index.

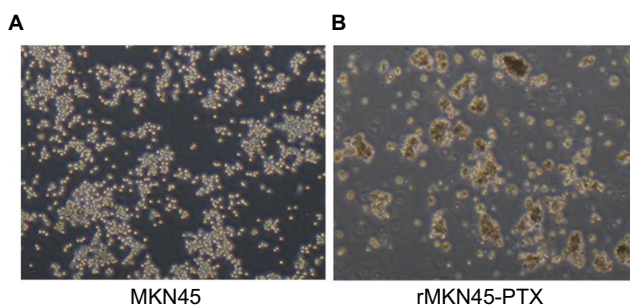


Figure 2 Morphologic differences between MKN45 (A) and rMKN45-PTX (B) under light microscope.

Note: rMKN45-PTX formed spheroid bodies (magnification $\times 40$).

Abbreviation: PTX, paclitaxel.

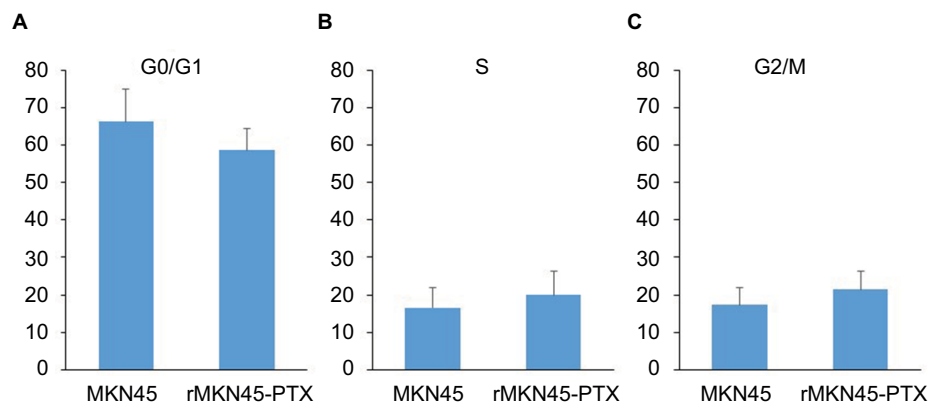


Figure 3 Cell cycle distribution.

Notes: There were no significant differences in the percentage of cells in G0/G1 phase (A) and G2/M phase (C) between rMKN45-PTX and MKN45 compared with S phase (B). Results are the mean of three experiments.

Abbreviation: PTX, paclitaxel.

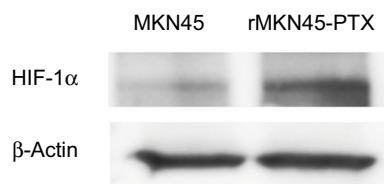


Figure 4 Western blot analyses of HIF-1 α . β -Actin was used as an internal control.

Note: Increased expression of HIF-1 α was observed in rMKN45-PTX cells.

Abbreviations: PTX, paclitaxel; HIF-1 α , hypoxia-inducible factor-1 alpha.

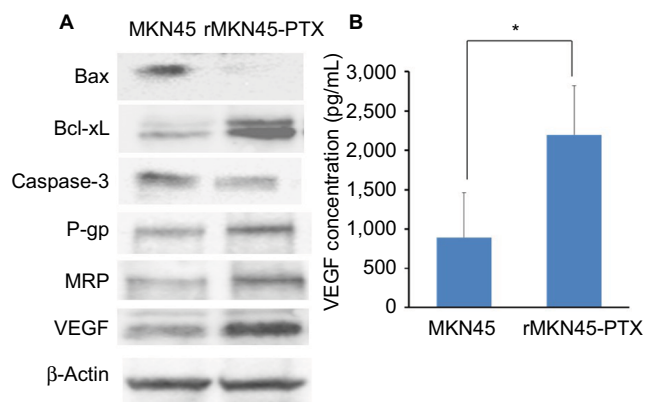


Figure 5 (A) Western blot analysis of Bax, Bcl-xL, caspase-3, P-gp, MRP, VEGF and β -actin in MKN45 and rMKN45-PTX. Expression of Bax and caspase-3 was significantly downregulated, whereas expression of Bcl-xL, P-gp, MRP and VEGF was increased in rMKN45-PTX. The average signal intensity was standardized to that of β -Actin. (B) VEGF levels in gastric cancer cells were measured by an ELISA system. **Notes:** Values represent mean \pm SD ($n = 3$). $*P < 0.05$.

Abbreviations: P-gp, P-glycoprotein; MRP, multidrug resistance-associated protein; VEGF, vascular endothelial growth factor; PTX, paclitaxel.

Tumor proliferation and progression

To examine proliferation and carcinogenesis of the drug-resistance cell line, we used a mouse xenograft model and evaluated the subcutaneous tumor volume. The time course of tumor growth is shown by the quantification of volume (Figure 7A and B). Tumors derived from rMKN45-PTX cells were significantly larger than those derived

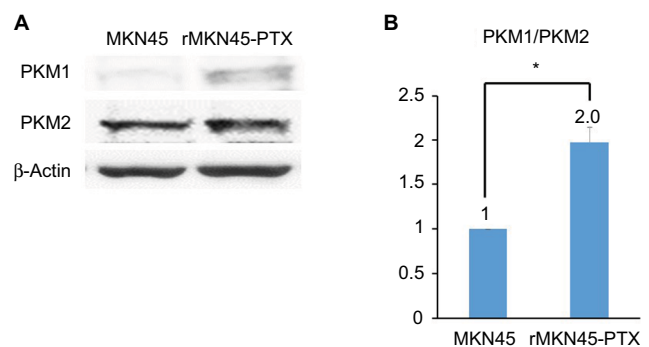


Figure 6 (A) Western blot analysis of PKM1 and PKM2. β -Actin was used as an internal control. (B) PKM1/PKM2 ratio calculated based on densitometric values of PKM1 and PKM2.

Notes: The PKM1/PKM2 ratio is presented relative to that of MKN45 cells (taken as 1.0). $*P < 0.05$.

Abbreviations: PKM, pyruvate kinase muscle; PTX, paclitaxel.

from MKN45 cells when measured at day 28 ($P < 0.05$). As shown in Figure 8, the number and size of peritoneal dissemination nodules tended to be larger in rMKN45-PTX-injected mice than in MKN45-injected mice. Both tumor number and weight were significantly higher in rMKN45-PTX mice.

Histological examination of xenograft tumors

NF- κ B immunoreactivity was increased in rMKN45-PTX tumors compared with MKN45 tumors (Figure 9A). VEGF expression in subcutaneous tumors derived from rMKN45-PTX cells was significantly higher than that in tumors from MKN45 cells (Figure 9A). Tumors from rMKN45-PTX exhibited increased expression of Ki-67 (Figure 9A and B) and PKM1, although the expression of PKM2 was almost the same in both tumors (Figure 9A). Peritoneal dissemination tumors showed the same pattern of expression (data not shown).

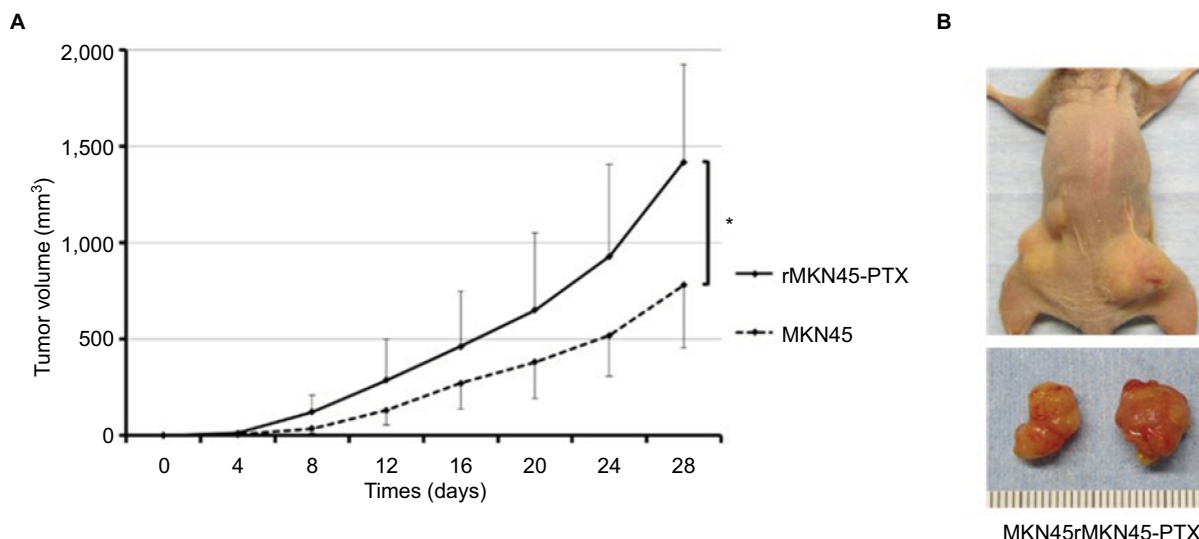


Figure 7 (A) Growth of tumors derived from rMKN45-PTX and MKN45. Tumor volume was measured every fourth day. **(B)** Representative images depicting the macroscopic appearance of the tumors at day 28.

Notes: Results are expressed as the mean \pm SD ($n = 5$). $*P < 0.05$.

Abbreviation: PTX, paclitaxel.

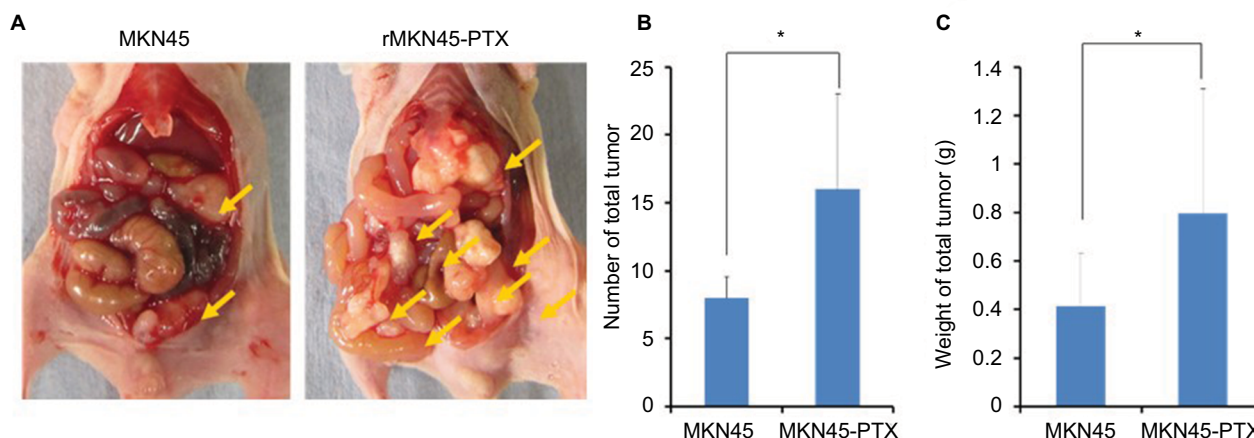


Figure 8 (A) Representative images depicting the macroscopic appearance of the tumors at day 14. Tumors were present in the peritoneal cavity (arrow). **(B)** Number and **(C)** weight (g) of disseminated nodules.

Notes: Results are mean \pm SD of five experiments. $*P < 0.05$.

Abbreviation: PTX, paclitaxel.

Discussion

Improving the efficacy of chemotherapy will require a better understanding of the mechanisms by which tumors become chemoresistant and development of strategies to overcome this resistance. The primary approach to this problem has been the establishment of chemoresistant cancer cell lines and identification of the underlying resistance mechanisms. In the present study, we established a PTX-resistant gastric cancer cell line (rMKN45-PTX) by stepwise exposure to PTX. The cell cycle distribution was similar in resistant and parental cell lines, but NF- κ B and HIF-1 α were over-expressed in rMKN45-PTX under normoxic conditions. Furthermore, we showed that the growth factor VEGF, the

antiapoptosis marker Bcl-xL, multidrug transporters P-gp and MDR, and the glycolytic enzyme PKM1 were upregulated in rMKN45-PTX. Consequently, rMKN45-PTX-derived tumors showed significantly enhanced proliferation and progression in subcutaneous and peritoneal dissemination models.

Our study showed that the cell cycle distribution was not related to acquisition of PTX resistance. Wang et al reported that cell cycle distribution may be an integral part of mechanisms responsible for chemoresistance.⁴ Furthermore, previous studies demonstrated that alteration of cell cycle distribution might be associated with chemoresistance to specific drugs including oxaliplatin and irinotecan, although no studies have demonstrated an association between taxan and cell cycle

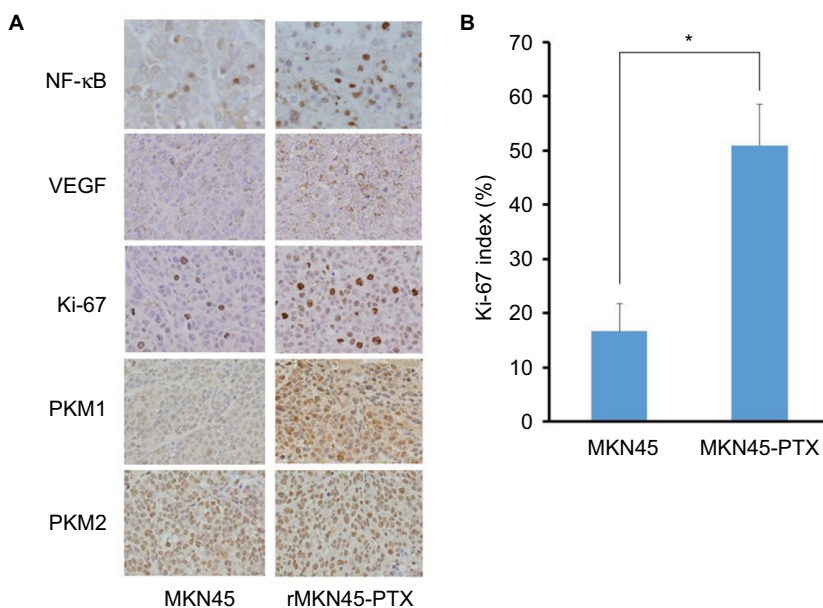


Figure 9 (A) Immunohistochemical examination of NF- κ B, VEGF, Ki-67, PKM1 and PKM2 in subcutaneous xenograft tumors (original magnification $\times 400$). **(B)** The Ki-67 index is shown as a percentage.

Notes: Results are mean \pm SD of five experiments. * $P < 0.05$.

Abbreviations: NF- κ B, nuclear factor kappa B; VEGF, vascular endothelial growth factor; PKM, pyruvate kinase muscle; PTX, paclitaxel.

distribution.¹⁸ These findings suggest that there may be a different mechanism underlying acquisition of PTX resistance.

In the present study, we showed that NF- κ B and HIF-1 α expression was increased during exposure of the parent cell line to PTX. Previous studies suggested that HIF-1 α might be a contributor to chemoresistance acquired by hypoxia and in part explain the increased level of intracellular HIF-1 α associated with resistance to therapy in head and neck, ovarian, esophageal, prostate and gastric cancer.^{15,19–22} However, HIF-1 α expression is induced not only in hypoxic conditions but also in non-hypoxic conditions and in response to other stressors such as chemotherapy and radiation.^{3,23} Also, Montagut et al demonstrated that NF- κ B activation was significantly correlated with chemoresistance and the number of breast cancer patients with NF- κ B activation increased after chemotherapy exposure.¹³

HIF-1 α is known to transcriptionally upregulate VEGF expression.^{10,24} In this study, we showed that VEGF was overexpressed in rMKN45-PTX cells by Western blotting, ELISA and immunohistochemistry. VEGF is a multifunctional cellular factor that can induce neovascularization and increase capillary permeability.^{25,26} As a result, the tumor vasculature shows an abnormal structure that is inefficient for oxygen and drug delivery.²⁷ Moreover, VEGF is one of the major factors that contributes to metastasis in various cancers, and VEGF overexpression has been associated with tumor progression and poor prognosis.^{10,28–30} We demonstrated

that rMKN45-PTX-derived tumors showed significantly enhanced tumor proliferation and progression in a subcutaneous model and a peritoneal dissemination model. In our clinical experience, patients with failure of cancer chemotherapy often rapidly develop tumor progression.

Apoptosis is an important mechanism for cell death following treatment with various types of chemotherapy. Caspase-3 is a proapoptotic effector enzyme that interacts with caspase-8 and caspase-9. Bax is a proapoptotic member of the Bcl-2 family that plays a key role in the induction of mitochondria-dependent apoptosis. By contrast, Bcl-xL is an antiapoptotic family member that can neutralize Bax function in the initiation of cell death. Overexpression of Bcl-xL protein occurs in many types of cancer cell and prevents cell death induced by anticancer drugs and radiation.³¹ Our findings demonstrated that the expression of Bcl-xL was markedly increased in rMKN45-PTX, which is in line with previous studies.^{32–34} The involvement of HIF-1 α in chemoresistance acquisition is possibly due to its role in the regulation of some apoptosis-related genes.

Accumulating evidence has shown that the mechanisms responsible for chemoresistance are associated with overexpression of two ATP-dependent drug transporter proteins, P-gp and MRP.^{35–37} These proteins act as ATP-dependent outward transport pumps and decrease the intracellular accumulation of drugs by reducing the cotransport mechanism of glutathione.³⁸ In particular, Sparreboom et al showed that

P-gp at the luminal side of the intestinal epithelium appears to be an important component of the defense against PTX, and P-gp was therefore associated with chemoresistance acquisition.³⁹ Furthermore, a previous study showed that HIF-1 α expression is correlated with MDR1/P-gp expression in colon carcinoma tissue and a colon cancer cell line.⁴⁰ We found that both P-gp and MRP were expressed in rMKN45-PTX, indicating that both P-gp and MRP were induced by HIF-1 α and play an important role in PTX transportation.

In the present study, we examined the association of pyruvate kinase muscle (PKM) and chemoresistance acquisition. PKM has two splicing variants: PKM1 is expressed in most normal tissues, whereas PKM2 is expressed in the embryonic stage cells and cancer cells.⁴¹ Recently, it was noted that cancer metabolism-related genes play an important role in chemoresistance acquisition. Especially, the Warburg effect has been reported in cancer cells.⁴² This phenomenon is that cancer cells use glycolysis for energy for energy production even when an adequate amount of oxygen is present.⁴² A previous study showed that PKM2 promotes the Warburg effect; the coordinated control of metabolism and proliferation by PKM2 is essential for tumorigenesis.^{43,44} As a result, it was previously thought that inhibitors and activators of PKM2 are well underway to evaluate their anticancer effects and suitability.⁴⁵ On the other hand, PKM1 promotes oxidase phosphorylation (OXPHOS).^{43,46} It was also reported that metabolic switching from glycolysis to OXPHOS contributes to chemoresistance acquisition.⁴⁷ Taniguchi et al reported that PKM2 was expressed in both parent and chemoresistant cells, whereas PKM1 was

commonly upregulated in various chemoresistant cells, and knockdown of PKM1 sensitized chemoresistant cells to chemotherapy.¹⁶ They concluded that PKM1 plays important roles in the chemoresistance acquisition of cancer cells.¹⁶ In the present study, we similarly demonstrated that PKM1 was upregulated in rMKN45-PTX cells in vivo and in vitro, although PKM2 was expressed in both cells. Their results suggested that PKM1 expression at the same time as PKM2 might be one of the key regulators of chemoresistance acquisition in gastric cancer.

There were several limitations to our study. First, we only evaluated one cell line and one chemotherapeutic agent. It is therefore necessary to evaluate other gastric cancer cell lines, other cancer types and other anticancer drugs. Second, we have no data on HIF-1 α knockdown in parental and chemoresistant cells using si-RNA specific for HIF-1 α . Third, we did not study the associated with HIF-1 α and PKM1 expression under conditions of chemotherapy. Nevertheless, this study demonstrated HIF-1 α expression in our chemoresistant cancer cell line and showed a relationship between PKM1 expression and chemoresistance.

Conclusion

rMKN45-PTX cells showed overexpression of HIF-1 α and enhanced tumor proliferation and progression. HIF-1 α is a key molecule in chemoresistance acquisition, most likely through its impact on angiogenesis, cell proliferation, apoptosis and multidrug transporters (Figure 10). Furthermore, PKM1 might also be important in chemoresistance acquisition. Further research into the relationship between

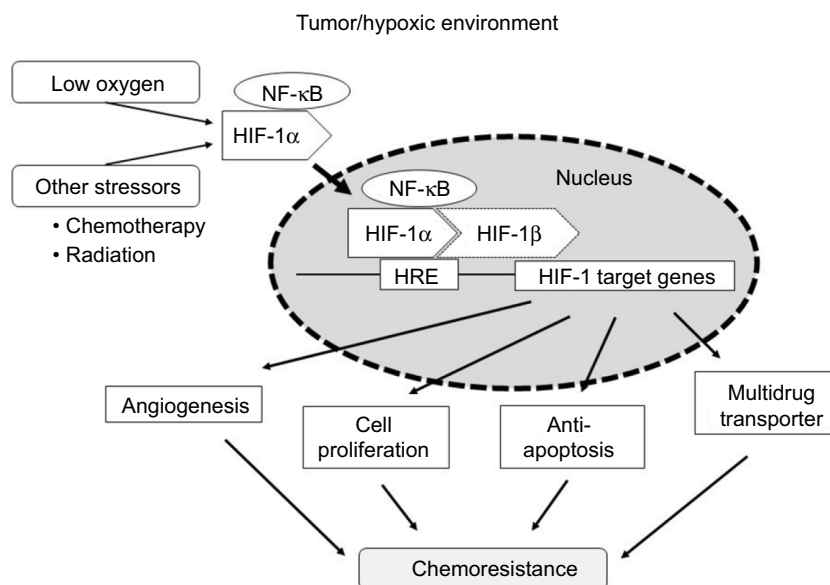


Figure 10 Scheme illustrating a chemoresistance mechanism involving HIF-1 α .

Abbreviations: HIF-1 α , hypoxia-inducible factor-1 alpha; HRE, hypoxic response element; NF- κ B, nuclear factor kappa B.

chemotherapy and chemoresistance may provide additional novel treatment strategies. In addition to inhibition of HIF-1 α , our data suggest that PKM1 might also be a target for tumor-specific molecular-based therapy.

Acknowledgments

We are grateful to members of the Department of Gastroenterological Surgery of Kanazawa University for their helpful suggestions. We thank Mary Derry, PhD ELS, from Edanz Group (www.edanzediting.com/ac) for editing a draft of this manuscript.

Disclosure

The authors report no conflicts of interest in this work.

References

- Orditura M, Galizia G, Sforza V, et al. Treatment of gastric cancer. *World J Gastroenterol*. 2014;20(7):1635–1649.
- Roth AD. Chemotherapy in gastric cancer: a never ending saga. *Ann Oncol*. 2003;14(2):175–177.
- Liu L, Ning X, Sun L, et al. Involvement of MGr1-Ag/37LRP in the vincristine-induced HIF-1 expression in gastric cancer cells. *Mol Cell Biochem*. 2007;303(1–2):151–160.
- Zhang X, Yashiro M, Qiu H, Nishii T, Matsuzaki T, Hirakawa K. Establishment and characterization of multidrug-resistant gastric cancer cell lines. *Anticancer Res*. 2010;30(3):915–921.
- Chung YM, Park S, Park JK, Kim Y, Kang Y, Yoo YD. Establishment and characterization of 5-fluorouracil-resistant gastric cancer cells. *Cancer Lett*. 2000;159(1):95–101.
- Qiu H, Yashiro M, Zhang X, Miwa A, Hirakawa K. A FGFR2 inhibitor, Ki23057, enhances the chemosensitivity of drug-resistant gastric cancer cells. *Cancer Lett*. 2011;307(1):47–52.
- Donaldson KL, Goolsby GL, Kiener PA, Wahl AF. Activation of p34cdc2 coincident with taxol-induced apoptosis. *Cell Growth Differ*. 1994;5(10):1041–1050.
- Gabizon A, Price DC, Huberty J, Bresalier RS, Papahadjopoulos D. Effect of liposome composition and other factors on the targeting of liposomes to experimental tumors: biodistribution and imaging studies. *Cancer Res*. 1990;50(19):6371–6378.
- Ward MW, Huber HJ, Weisová P, Düssmann H, Nicholls DG, Prehn JH. Mitochondrial and plasma membrane potential of cultured cerebellar neurons during glutamate-induced necrosis, apoptosis, and tolerance. *J Neurosci*. 2007;27(31):8238–8249.
- Stoeltzing O, McCarty MF, Wey JS, et al. Role of hypoxia-inducible factor 1 α in gastric cancer cell growth, angiogenesis, and vessel maturation. *J Natl Cancer Inst*. 2004;96(12):946–956.
- McMahon S, Grondin F, McDonald PP, Richard DE, Dubois CM. Hypoxia-enhanced expression of the proprotein convertase furin is mediated by hypoxia-inducible factor-1: impact on the bioactivation of proproteins. *J Biol Chem*. 2005;280(8):6561–6569.
- Muñoz-Nájara UM, Neurath KM, Vumbaca F, Claffey KP. Hypoxia stimulates breast carcinoma cell invasion through MT1-MMP and MMP-2 activation. *Oncogene*. 2006;25(16):2379–2392.
- Montagut C, Tusquets I, Ferrer B, et al. Activation of nuclear factor-kappa B is linked to resistance to neoadjuvant chemotherapy in breast cancer patients. *Endocr Relat Cancer*. 2006;13(2):607–616.
- Rius J, Guma M, Schachtrup C, et al. NF-kappaB links innate immunity to the hypoxic response through transcriptional regulation of HIF-1 alpha. *Nature*. 2008;453(7196):807–811.
- Liu L, Ning X, Sun L, et al. Hypoxia-inducible factor-1 alpha contributes to hypoxia-induced chemoresistance in gastric cancer. *Cancer Sci*. 2008;99(1):121–128.
- Taniguchi K, Sakai M, Sugito N, et al. PKM1 is involved in resistance to anti-cancer drugs. *Biochem Biophys Res Commun*. 2016;473(1):174–180.
- Okazaki M, Fushida S, Harada S, et al. The angiotensin II type 1 receptor blocker candesartan suppresses proliferation and fibrosis in gastric cancer. *Cancer Lett*. 2014;355(1):46–53.
- Donaldson KL, Goolsby GL, Wahl AF. Cytotoxicity of the anticancer agents cisplatin and taxol during cell proliferation and the cell cycle. *Int J Cancer*. 1994;57(6):847–855.
- Quintero M, Mackenzie N, Brennan PA. Hypoxia-inducible factor 1 (HIF-1) in cancer. *Eur J Surg Oncol*. 2004;30(5):465–468.
- Russell DL, Ian S, Adrian L. The role of hypoxia-inducible factor-1 in three-dimensional tumor growth, apoptosis, and regulation by the insulin-signaling pathway. *Cancer Res*. 2005;65(10):4147–4152.
- Um JH, Kang CD, Bae JH, et al. Association of DNA-dependent protein kinase with hypoxia inducible factor-1 and its implication in resistance to anticancer drugs in hypoxic tumor cells. *Exp Mol Med*. 2004;36(3):233–242.
- Semenza GL. Signal transduction to hypoxia-inducible factor 1. *Biochem Pharmacol*. 2002;64(5–6):993–998.
- Harada H, Inoue M, Itasaka S, et al. Cancer cells that survive radiation therapy acquire HIF-1 activity and translocate towards tumour blood vessels. *Nat Commun*. 2012;3:783.
- Kitajima Y, Miyazaki K. The critical impact of HIF-1 α on gastric cancer biology. *Cancers (Basel)*. 2013;5(1):15–26.
- Connolly DT, Heuvelman DM, Nelson R, et al. Tumor vascular permeability factor stimulates endothelial cell growth and angiogenesis. *J Clin Invest*. 1989;84(5):1470–1478.
- Leung DW, Cachianes G, Kuang WJ, Goeddel DV, Ferrara N. Vascular endothelial growth factor is a secreted angiogenic mitogen. *Science*. 1989;246(4935):1306–1309.
- Trédan O, Lacroix-Triki M, Guiu S, et al. Angiogenesis and tumor microenvironment: bevacizumab in the breast cancer model. *Target Oncol*. 2015;10(2):189–198.
- Chen WT, Huang CJ, Wu MT, Yang SF, Su YC, Chai CY. Hypoxia-inducible factor 1 alpha is associated with risk of aggressive behavior and tumor angiogenesis in gastrointestinal stromal tumor. *Jpn J Clin Oncol*. 2005;35(4):207–213.
- Mizokami K, Kakeji Y, Oda S, et al. Clinicopathological significance of hypoxia-inducible factor 1 alpha overexpression in gastric carcinomas. *J Surg Oncol*. 2006;94(2):149–154.
- Fukuda R, Kelly B, Semenza GL. Vascular endothelial growth factor gene expression in colon cancer cells exposed to prostaglandin E2 is mediated by hypoxia-inducible factor 1. *Cancer Res*. 2003;63(9):2330–2334.
- Bargou RC, Wagener C, Bommert K, et al. Overexpression of the death-promoting gene Bax-alpha which is downregulated in breast cancer restores sensitivity to different apoptotic stimuli and reduces tumor growth in SCID mice. *J Clin Invest*. 1996;97(11):2651–2659.
- Crawford A, Nahta R. Targeting Bcl-2 in herceptin-resistant breast cancer cell lines. *Curr Pharmacogenomics Person Med*. 2011;9(3):184–190.
- Shajahan AN, Dobbin ZC, Hickman FE, Dakshnamurthy S, Clarke R. Tyrosine phosphorylated caveolin-1 (Tyr-14) increases sensitivity to paclitaxel by inhibiting BCL2 and BCLxL proteins via c-Jun N-terminal kinase (JNK). *J Biol Chem*. 2012;287(21):17682–17692.
- Zhao Q, Tan BB, Li Y, Fan LQ, Yang PG, Tian Y. Enhancement of drug sensitivity by knockdown of HIF-1 α in gastric carcinoma cells. *Oncol Res*. 2016;23(3):129–136.
- Endo K, Maehara Y, Kusumoto T, Ichiyoshi Y, Kuwano M, Sugimachi K. Expression of multidrug-resistance-associated protein (MRP) and chemosensitivity in human gastric cancer. *Int J Cancer*. 1996;68(3):372–377.
- Fan K, Fan D, Cheng LF, Li C. Expression of multidrug resistance-related markers in gastric cancer. *Anticancer Res*. 2000;20(6C):4809–4814.

37. Zhao Y, Xiao B, Chen B, Qiao T, Fan D. Upregulation of drug sensitivity of multidrug-resistant SGC7901/VCR human gastric cancer cells by bax gene transduction. *Chin Med J (Engl)*. 2000;113(11):977–980.
38. Xu HW, Xu L, Hao JH, Qin CY, Liu H. Expression of P-glycoprotein and multidrug resistance-associated protein is associated with multidrug resistance in gastric cancer. *J Int Med Res*. 2010;38(1):34–42.
39. Sparreboom A, van Asperen J, Mayer U, et al. Limited oral bioavailability and active epithelial excretion of paclitaxel (Taxol) caused by P-glycoprotein in the intestine. *Proc Natl Acad Sci U S A*. 1997;94(5):2031–2035.
40. Chen J, Ding Z, Peng Y, et al. HIF-1 α inhibition reverses multidrug resistance in colon cancer cells via downregulation of MDR1/P-glycoprotein. *PLoS One*. 2014;9(6):e98882.
41. Christofk HR, Vander Heiden MG, Wu N, Asara JM, Cantley LC. Pyruvate kinase M2 is a phosphotyrosine-binding protein. *Nature*. 2008;452(7184):181–186.
42. Vander Heiden MG, Cantley LC, Thompson CB. Understanding the Warburg effect: the metabolic requirements of cell proliferation. *Science*. 2009;324(5930):1029–1033.
43. Chen M, Zhang J, Manley JL. Turning on a fuel switch of cancer: hnRNP proteins regulate alternative splicing of pyruvate kinase mRNA. *Cancer Res*. 2010;70(22):8977–8980.
44. Yang W, Xia Y, Ji H, et al. Nuclear PKM2 regulates β -catenin transactivation upon EGFR activation. *Nature*. 2011;480(7375):118–122.
45. Tamada M, Suematsu M, Saya H. Pyruvate kinase M2: multiple faces for conferring benefits on cancer cells. *Clin Cancer Res*. 2012;18(20):5554–5561.
46. Christofk HR, Vander Heiden MG, Harris MH, et al. The M2 splice isoform of pyruvate kinase is important for cancer metabolism and tumour growth. *Nature*. 2008;452(7184):230–233.
47. Wolf DA. Is reliance on mitochondrial respiration a “chink in the armor” of therapy-resistant cancer? *Cancer Cell*. 2014;26(6):788–795.

Cancer Management and Research

Publish your work in this journal

Cancer Management and Research is an international, peer-reviewed open access journal focusing on cancer research and the optimal use of preventative and integrated treatment interventions to achieve improved outcomes, enhanced survival and quality of life for the cancer patient. The manuscript management system is completely online and includes

Submit your manuscript here: <https://www.dovepress.com/cancer-management-and-research-journal>

a very quick and fair peer-review system, which is all easy to use. Visit <http://www.dovepress.com/testimonials.php> to read real quotes from published authors.

Dovepress